Revista Mexicana de Física S **58** (2) 221–224 DICIEMBRE 2012

Displacements of hysteresis loops in magnetite nanoparticles

J. Mazo-Zuluaga[a], J. Mejía-López[b], F. Muñoz[c], and J. Restrepo[a]
[a]*Instituto de Física, Universidad de Antioquia, A.A. 1226 Medellín, Colombia.*
[b]*Facultad de Física, Pontificia Universidad Católica de Chile, Santiago de Chile, Chile.*
[c]*Facultad de Física, Universidad de Chile, Santiago de Chile, Chile.*
e-mail: johanmazo@gmail.com

Recibido el 25 de junio de 2010; aceptado el 11 de octubre de 2010

In this work we present a Monte Carlo study to address the effect of surface anisotropy on the exchange bias behavior in magnetite nanoparticles. Our theoretical framework is based on a three-dimensional classical Heisenberg model with nearest magnetic neighbor interactions involving realistic crystalline structure for magnetite with tetrahedral and octahedral irons. Cubic magnetocrystalline anisotropy for core spins, single-ion site anisotropy for surface spins, and interaction with a uniform external magnetic field, were considered. Our results revealed the onset of low temperature exchange bias field at high enough values of the surface anisotropy constant (K_S). Our results indicate also that the strongly pinned spins at high enough surface anisotropy values are responsible for both the horizontal and vertical shifts of the hysteresis loops.

Keywords: Magnetite nanoparticles; magnetocrystalline anisotropy; hysteresis loops.

En este trabajo presentamos un estudio Monte Carlo para explorar el efecto de la anisotropía de superficie sobre el comportamiento magnético y de exchange bias en nanopartículas de magnetita. Nuestro marco teórico se basa en un modelo de Heisenberg clásico tridimensional con interacción a primeros vecinos magnéticos y una estructura cristalina realista para la magnetita tomando en cuenta los sitios de hierro tetraedrales y octaedrales. Se considera la anisotropía cúbica magnetocrsitalina para los espines internos, una anisotropía superficial para los espines pertenecientes a la superficie, y la interacción de los espines con un campo magnético uniforme externo a la muestra por medio de un término Zeemann. Los resultados revelan la aparición del campo de exchange bias en el régimen de baja temperatura para valores suficientemente altos de la constante de anisotropía de superficie K_S. Se hace evidente también que los espines de superficie fuertemente anclados, a valores altos de anisotropía superficial, son responsables de los desplazamientos, tanto horizontales como verticales, de los ciclos de histéresis.

Descriptores: Nanopartículas de magnetita; anisotropía magnetocristalina; ciclos de histéresis.

PACS: 75.75.+a; 75.30.Gw; 75.70.Rf; 75.50.Gg; 75.40.Mg; 75.10.Hk; 75.30.Et

1. Introduction

Although fine particles were the first type of system where exchange bias was observed it is interesting to note that most of the work on particles deals with some cases consisting of a ferromagnetic core surrounded by its respective antiferromagnetic or ferrimagnetic native oxide [1-3], and very few studies on pure systems exhibiting exchange bias (*e.g.* pure ferrimagnetic and antiferromagnetic nanoparticles) have been carried out [4].

Focusing our attention on magnetite Fe_3O_4 as a pure system is valid to mention that exchange bias and surface spin-glass-like behaviors have been reported to occur in Fe_3O_4 nanoparticles compacted under high pressure. In this case the hysteresis loop is shifted due to the exchange coupling between the core spins and the surface spins, which behave as a spin-glass-like phase [5]. Considering some studies suggesting the occurrence of a "surface spin-glass-like state", it is found they are consistent with a surface spin disordered layer freezing below certain low temperature and behaving in an entirely different manner from the core. Such a spin-glass-like surface can be thought, in analogy with layered systems, as playing the role of an "AFM" layer surrounding a ferrimagnetic core. However, even though this intuitive picture can seem simple, a full understanding of the exchange bias properties of pure nanoparticles seems to be beyond standard exchange bias models.

Concerning magnetite nanoparticles, it is worth noting they possess some of the features needed for the occurrence of shifted hysteresis loops. On the one hand, the presence of competing interactions can lead to magnetic frustration on the surface due to under-coordination. In magnetite different superexchange integrals, namely $J_{AA} < 0$, $J_{AB} < 0$ and $J_{BB} > 0$, are present. The intersublattice superexchange interaction J_{AB}, which is antiferromagnetic, is dominant and it contributes to the appearance of ferrimagnetic order [6,7]. Since such superexchange interactions are mediated by an intervening oxygen ion, exchange bonds are broken if an oxygen is missing from the surface, and, consequently, electrons can no longer participate in the superexchange. In principle, this can lead to anisotropy, which, in turn, can be either perpendicular or parallel to the surface depending on the sign of the crystal-field interaction.

On the other hand, chemical surface modification can also induce changes in the surface anisotropy and exchange bias properties. Several works indicating such kind of strong magnetic surface effects depending on the coating medium have also been addressed [8,9]. Different facts point out to the surface of magnetite at nanoscale behaving in an entirely different manner than bulk magnetite. Surface studies in mag-

netite thin films showed the influence of surface morphology, roughness, and stoichiometric inhomogeneities on the electronic structure [10]. Ab-initio calculations by employing density functional theory DFT revealed that either metallic or half-metallic (as in bulk magnetite) behavior can be found depending on the particular cation distribution on the surface [11]. A half-metal to metal transition at the (100) Fe_3O_4 surface has been identified by means of spin-resolved photoemission experiments on thin films [12] and has been confirmed as well by using first-principles calculations [13].

Hence, it is clear that the matrix where particles can be embedded, the coating medium surrounding the surface of the particles, or even the specific way by which the particle surface ends at atomic level, can act as important sources of surface anisotropy. These interesting issues have motivated us to explore the effect of the surface anisotropy constant as a driving force for giving rise to exchange bias in pure ferrimagnetic nanoparticles.

2. Model and computational details

The model employed in this study reproduces in realistic way the inverse spinel crystalline structure of magnetite (Fe_3O_4 -space group Fd3m) with 56 ions per cubic unit cell distributed as follows: 32 O^{2-} oxygen ions, 8 Fe^{3+} iron ions in tetrahedral sites (A-sites), and finally 8 Fe^{2+} and 8 Fe^{3+} ions randomly located in octahedral sites (B-sites). Magnetic moments of iron ions were represented by classical Heisenberg spins. Their magnitudes have been considered taking into account their respective valence states and therefore their corresponding electronic configurations. Thus, a value of $S = 5/2$ was used for Fe^{3+} and $S = 2$ for Fe^{2+}. Oxygen ions were considered as non-magnetic. Numerical values of the coupling integrals employed were $J_{AA} = -0.11$ meV, $J_{BB} = +0.63$ meV, and $J_{AB} = -2.92$ meV [6]. Hence, the sign and greater magnitude of the inter-sublattice integral J_{AB} accounts for antiparallel intersublattice alignment. This fact, in addition to the different spin values, explains the ferrimagnetic behavior observed in bulk magnetite below the Curie temperature. The classical Heisenberg Hamiltonian describing our system reads:

$$\begin{aligned} H = & -2\sum_{\langle i,j\rangle} J_{ij}\vec{S}_i\cdot\vec{S}_j \\ & - K_V\sum_i \left(S_{x,i}^2S_{y,i}^2 + S_{y,i}^2S_{z,i}^2 + S_{x,i}^2S_{z,i}^2\right) \\ & - K_V\sum_k \left(S_k\vec{e}_k\right)^2 - g\mu_B\vec{H}\cdot\sum_i\vec{S}_i \end{aligned} \quad (1)$$

The first sum involves nearest magnetic neighbors interactions. The number of terms in this sum depends on the coordination numbers. Under bulk conditions three different coordination numbers are identified: $z_{AA} = 4$, $z_{BB} = z_{BA} = 6$, and $z_{AB} = 12$. These numbers apply for the core, whereas the surface has been defined as formed by iron ions having coordination numbers smaller than those corresponding to bulk conditions. The second term in Eq. (1) is the core cubic magnetocrystalline anisotropy and K_V (=0.002 meV/spin) is the first-order bulk anisotropy constant [14]. The third term accounts for the single-ion site surface anisotropy where the unitary vector $\boldsymbol{e}_k$ is computed on every k-th position taking into account the positions $\boldsymbol{P}_j$ of the nearest magnetic neighbors [15].

$$\bar{e}_k = \frac{\sum_j\left(\vec{P}_k - \vec{P}_j\right)}{\left|\sum_j\left(\vec{P}_k - \vec{P}_j\right)\right|} \quad (2)$$

Positions over which these vectors were computed correspond exclusively to Fe-cations on the surface. The last term in Eq. (1) gives the interaction of spins with a uniform external magnetic field. Dipolar interactions were neglected in the present study regarding its small contribution ($\sim 10^{-5}$ meV/spin) compared to the surface anisotropy contribution ($\sim 10^{-2}$ meV/spin); see Ref. [16].

Regarding the Monte Carlo simulation, we have employed a single-spin movement Metropolis dynamics. Averages were computed over 25 different samples corresponding to five different magnetic starting configurations and five different realizations of Fe^{3+} and Fe^{2+} ions at octahedral sites per each initial magnetic configuration. A maximum number of 5×10^5 Monte Carlo steps per spin (MCS) were used and the first 2×10^5 steps were discarded for equilibration. Numerical values for the K_S/K_V ratio were taken to range between 1 and 10^4. Such extreme values allow: (i) to determine the stability of the magnetic structures involved, and (ii) to model different experimental and likely scenarios where a given matrix or coating medium, such as an organic surfactant, can effectively change the surface anisotropy. Nearly spherical nanoparticles of different diameters were considered: $2 < D < 7$ nm. Free boundary conditions were implemented and the thermodynamic quantities computed were the energy, specific heat, the magnetization per spin, the magnetic susceptibility, and their respective contributions arising from core, surface, and A and B sites.

3. Results and discussion

At small K_S/K_V values (around 10) and low temperature regime nanoparticles are found in a ferrimagnetic monodomain state as in the bulk case. Loops (not shown) are characterized by a high degree of squareness, and a marked tendency of the saturation magnetization and the remanence to decrease as the particle size decreases. These features imply a reversal of the magnetization as a whole with a well-defined ferrimagnetic moment, *i.e.* nanoparticles behave like macrospins, in similar way as in the Stoner-Wohlfarth model [16]. Under bulk conditions the saturation magnetization per spin goes to 2/3 accordingly with stoichiometry and the different Fe spin values involved. Values close to this limit were obtained for the biggest nanoparticles studied, of 6

and 7 nm in diameter, whereas finite size effects become evident for smaller nanoparticles having smaller values of the saturation magnetization per spin. Here, magnetization reduction is due to uncompensated spins on the surface and not to a surface spin canting phenomenology. Concerning exchange bias properties at these low K_S values no shifted loops can be confirmed within the degree of precision provided by the error bars.

As the surface anisotropy increases hysteresis loops become substantially different, they remain symmetric but different from those cycles at smaller surface anisotropy values, and now appear less square and more elongated. Remanence reduction becomes more remarkable as the particle size decreases. This fact is mainly due to a small tendency of the surface spins to be pinned along radial directions for which magnetic structures are of the throttled type, where is more noticeable the tendency of surface spins to be perpendicular to the tangent plane on each site on the surface as the surface anisotropy increases [17-19]. For greater surface anisotropy values beyond certain threshold, which depends on the system size, magnetic structures become of the hedgehog type with magnetization close to zero. Hysteresis loops are now characterized by steps or jumps, which become more pronounced as the surface anisotropy increases (Fig. 1). Such jumps are attributed to the high degree of spin pinning, for which reversal does not occur in a continuous fashion, and to a discrete shift in the center of symmetry of the magnetic moment distribution in the direction opposite to the field [17].

Inset in Fig. 1 shows the dependence of exchange bias as a function of K_S/K_V. As can be observed, for intermediate values of the ratio K_S/K_V negative exchange bias is observed, whereas for higher values of this ratio exchange bias becomes positive. Finally, for huge values of K_S/K_V the hedgehog-type magnetic structure becomes practically rigid giving rise to the absence of exchange bias.

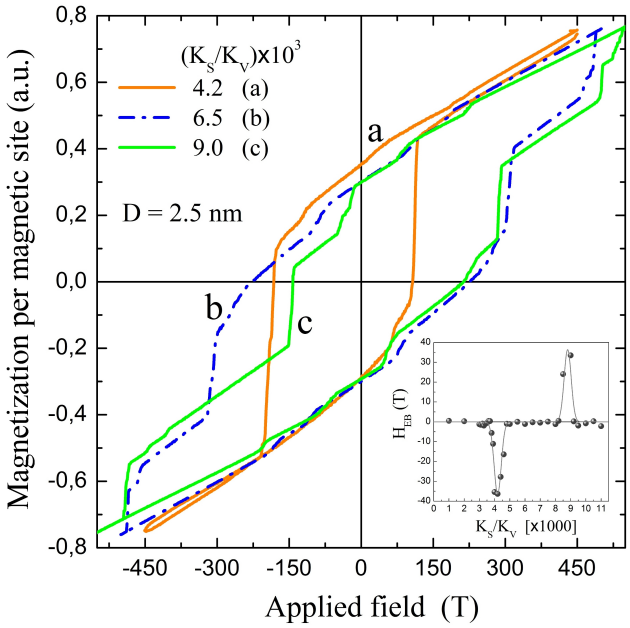

FIGURE 1. Shifted hysteresis loops for 2.5 nm diameter nanoparticles and some selected K_S/K_V values beyond 3000. Inset shows the surface anisotropy dependence of exchange bias field.

As is well established, in order to generate exchange bias it is necessary the presence of at least two exchange-coupled phases: a reversible phase whose magnetic moments can be reversed and a fixed phase whose moments can not be reversed. In our case those pinned spins, which belong to the surface or even to the core, play the role of the fixed phase. On the other hand, the reversible phase includes both the contributions of the core and the reversible part of the surface. The relative proportion of each phase will depend on the magnitude of the surface anisotropy. This hard-soft interplay between surface and core, which can be observed in Fig. 2, gives rise to the occurrence of an interface across which surface and core spins interact via superexchange couplings. On the other hand, uncompensated spins on the surface, where different spin values are involved, are not necessarily symmetrically distributed due to the finiteness and discreteness of the system. This fact is more evident for smaller nanoparticles. Such spins, strongly pinned, tend to exert a microscopic torque on the core spins. Once the field is applied some of those torques become favored, depending on the direction along which the field is applied. As a result, and due to the non-symmetric distribution of such torques, a hystere-

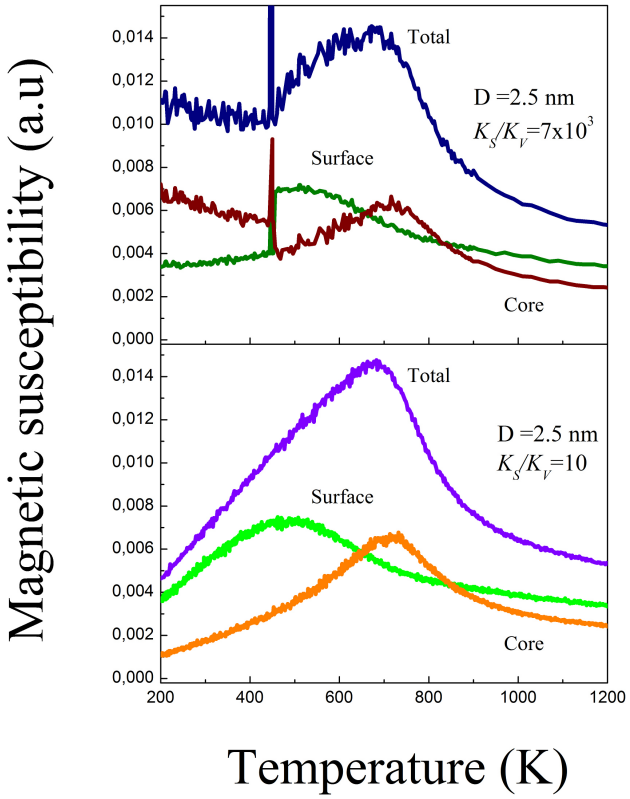

FIGURE 2. Thermal dependence of the magnetic susceptibility for D=2.5 nm and two K_S/K_V values. Surface and core contributions are shown explicitly, indicating clearly a hard-soft interplay between core and surface. The sharp peak at the top panel is attributed to the transition to the hedgehog structure.

sis loop shift will be observed along the field axis. Similar mechanisms for explaining exchange bias properties have been suggested as well to occur in oxide-coated manganese nanoparticles [18].

In short, as the surface anisotropy increases the magnetization reversal process becomes progressively gradual. For K_S/K_V ratios above certain threshold value of approximately 5×10^3, several features are remarkable:

(i) Loops are widely elongated and open up to approximately the maximum applied field,

(ii) magnetization reversal occurs by steps, suggesting a distribution of switching fields or rotational barriers, and

(iii) exchange bias properties appear.

Once the field is applied on a hedgehog-type nanoparticle very high fields are required to force transitions of surface spins and to overcome the high degree of pinning of the magnetic moments. Exchange bias and the presence of jumps during magnetization reversal is attributed to the high degree of surface spin pinning, which is relevant at high enough surface anisotropy values above the threshold, when such behavior tends to propagate through the core via superexchange couplings. Shifts in both horizontal and vertical directions, with some similarities to the loops shifts studied here, have also been found experimentally in other systems [20,21].

4. Conclusions

The effect of surface anisotropy and particle size on the hysteretic and magnetic properties of magnetite nanoparticles has been addressed. Results revealed that the surface anisotropy can act as a driving force giving rise to the occurrence of a strong surface spin pinning. The tendency of the surface spins to be more or less compensated, depending on the particle size, in addition to the different ratio of octahedral to tetrahedral spins, explains why the values of surface anisotropy for which exchange bias appears are different for different system sizes. The pinning mechanism is also the one responsible for magnetization and remanence reduction. Susceptibility data, computed separately for the core and the surface, suggest a magnetically harder character for the surface relative to the core; such differences are K_S-driven and depend on the system size. Such a hard-soft interplay, via the surface anisotropy, is the proposed mechanism for explaining the observed exchange bias phenomenology. It is worth to mention that, as part of this systematic study on iron oxides, a study on the relaxation of surface atoms is currently been carried out in order to explore the effect of this surface relaxation on the magnetic properties of the studied samples.

Acknowledgements

This work was supported by: Colombia-Chile Scientific Cooperation Program under contracts Nos. 279-2009(Colciencias) and 2008-157(Conicyt); CODI-Sostenibilidad project of GES at Universidad de Antioquia-Colombia; and Fondecyt-Chile Grant No. 1100365.

1. M. Spasova *et al.*, *J. Magn. Magn. Mater.* **272-276** (2004) 1508.
2. D.S. Geoghegan, P.G. McCormick, and R. Street, *Mater. Sci. Forum* **179-181** (1995) 629.
3. C.M. Hsu, H.M. Lin, and K.R. Tsai, *J. Appl. Phys.* **76** (1994) 4793.
4. R.H. Kodama, A.E. Berkowitz, E.J. McNiff, Jr., and S. Foner, *J. Appl. Phys*. **81** (1997) 5552.
5. H. Wang *et al.*, *Phys. Rev. B* **70** (2004) 092409.
6. M. Uhl, and B. Siberchicot, *J. Phys.: Condens. Matter* **7** (1995) 4227.
7. C.M. Srivastava, G. Srinivasan, and N.G. Nanadikar, *Phys. Rev. B* **19** (1979) 499.
8. Y. Koseoglu, *J. Magn. Magn. Mater.* **300** (2006) e327.
9. A.F. Bakuzis, A.R. Pereira, J.G. Santos, and P.C. Morais, *J. Appl. Phys.* **99** (2006) 08C301.
10. K. Jordan *et al.*, *Phys. Rev. B* **74** (2006) 085416.
11. L. Zhu, K.L. Yao, and Z.L. Liu, *Phys. Rev. B* **74** (2006) 035409.
12. M. Fonin *et al.*, *Phys. Rev. B* **72** (2005) 104436.
13. C. Cheng, *Phys. Rev. B* **71** (2005) 052401.
14. G.F. Goya, T.S. Berquo, F.C. Fonseca and M.P. Morales, *J. Appl. Phys.* **94** (2003) 3520.
15. R.H. Kodama and A.E. Berkowitz, *Phys. Rev. B* **59** (1999) 6321.
16. H. Kachkachi and M. Dimian, *Phys. Rev. B* **66** (2002) 174419.
17. P.Z. Si *et al.*, *Appl. Phys. Lett.* **87** (2005) 133122.
18. Y. Labaye, O. Crisan, L. Berger, J.M. Grenèche, and J.M.D. Coey, *J. Appl. Phys.* **91** (2002) 8715.
19. J. Mazo-Zuluaga, J. Restrepo, and J. Mejía-López, *J. Appl. Phys.* **103** (2008) 113906.
20. A. Mumtaz, K. Maaz, B. Janjua, S.K. Hasanain, and M.F. Bertino, *J. Magn. Magn. Mater.* **313** (2007) 266.
21. R.K. Zheng, G.H. Wen, K.K. Fung, and X.X. Zhang, *Phys. Rev. B* **69** (2004) 214431.